Experimental assessment of an innovative strengthening material for brick masonry infills

A. Martins[1], G. Vasconcelos[1], R. Fangueiro[2], F. Cunha[2]

[1] *ISISE, Department of Civil Engineering, University of Minho, Azurém, P-4800-058 Guimarães, Portugal. Tel: +351 253 510 200, Fax: +351 253 510 217*

[2] *2C2T, Department of Civil Engineering, University of Minho, Azurém, P-4800-058 Guimarães, Portugal. Tel: +351 253 510 200, Fax: +351 253 510 217*

Corresponding author: *graca@civil.uminho.pt*

Abstract

The vulnerability of masonry infill walls has been highlighted in recent earthquakes in which severe in-plane damage and out-of-plane collapse developed, justifying the investment in the proposal of strengthening solutions aiming to improve the seismic performance of these construction elements. Therefore, this work presents an innovative strengthening solution to be applied in masonry infill walls, in order to avoid brittle failure and thus minimize the material damage and human losses. The textile-reinforced mortar technique (TRM) has been shown to improve the out-of-plane resistance of masonry and to enhance its ductility, and here an innovative reinforcing mesh composed of braided composite rods is proposed. The external part of the rod is composed of braided polyester whose structure is defined so that the bond adherence with mortar is optimized. The mechanical performance of the strengthening technique to improve the out-of-plane behaviour of brick masonry is assessed based on experimental bending tests. Additionally, a comparison of the mechanical behaviour of the proposed meshes with commercial meshes is provided. The idea is that the proposed meshes are efficient in avoiding brittle collapse and premature disintegration of brick masonry during seismic events.

Keywords: Masonry infills, seismic retrofitting, carbon fibres, glass fibres, textile braided rod meshes

1 Introduction

Several past seismic events in southern Europe have highlighted the vulnerability of the very common constructive solution of enclosure brick masonry walls. This construction element is very common in reinforced concrete buildings and also in steel buildings [1]. The masonry infills present out-of-plane failure mechanisms, which are characterized as being brittle and thus considered as undesirable due to the high cost involved in repair/reconstruction and to the risk to human safety [2-4]. Generally, the behaviour of the walls depends on the resistance, stiffness and slenderness of the panel and its interaction with the surrounding frame. For decades, these elements have been considered as nonstructural and therefore there are no specific guidelines for their design [2]. Besides, the constructive details in the daily design of buildings are almost non-existent. In this respect, Eurocode 8 (2004) [5] provides some recommendations about the construction of masonry infill walls to improve their in-plane and out-of-plane behaviour and to avoid their brittle failure and premature disintegration, including: (1) the addition of light wire meshes well anchored on one face of the wall; (2) wall ties fixed to the columns and cast into the bedding planes of the masonry; (3) concrete posts and belts across the panels and through the full thickness of the wall.

This means that there is a large segment within the building stock in seismic-prone areas that needs to undergo preventive actions, particularly for out-of-plane loads. This can range from simple connection of the masonry infills to the frame structures, which can also be applied to the case of already damaged elements, to the strengthening of the masonry infills. The potential benefits of strengthening the masonry infills go beyond the stability of these nonstructural elements, as this can improve also the behaviour of the whole structure when faced with seismic events [6].

The strengthening solutions for masonry infill walls may be varied and there has been an evolution with respect to methods and materials. Laminated fibre-reinforced polymer (FRP) strengthening is a viable retrofitting technique due to its small thickness, advantageous strength/weight ratio, high stiffness, and because it is relatively easy to apply. This material was firstly applied in concrete structures by bonding external polymer sheet to the surface (EBR technique) or by introducing the laminated fibers into slots (near surface-mounted technique) in the concrete [7]. However, these materials also have disadvantages like inadequate bonding of the reinforcement to the masonry, resulting often in the detachment of the reinforcement relative to the support. An alternative retrofitting technique that has been studied is based on meshes of fibres embedded in cementitious matrix materials, commonly referred to as Textile-Reinforced Mortar (TRM). This technique may provide several advantages such as the overcoming of bond weakness and problems with humidity [8]. In this respect, optimization of the textile meshes inserted in masonry mortar with the aim of improving the tensile strength of the walls and the deformation capacity, resulting in a more ductile failure, has been investigated [8-9]. Several authors [10-17] have analysed the bending and shear behaviour of strengthened masonry walls, varying the number of layers of the reinforcing materials applied in both sides, the typology of the reinforcement (glass mesh, carbon mesh, basalt mesh, propylene mesh and polyester mesh), alternative bonding materials like epoxy resin, and the load level of compression applied in the samples. Based on the response of masonry walls subjected to cyclic out-of-plane loading, it was concluded that the TRM technique results in great benefit to the strength and particularly to the deformation capacity. This enhanced mechanical behaviour under flexure is attributed to the tensile resistance of the reinforced mortar, the failure being controlled by failure of the fibre or by sliding of the mesh or fibres from the mortar. Even weak TRM solutions ("low-tech" textiles

combined with low resistance), when properly placed, result in a major increase in the resistance and deformation capacity in walls submitted to out-of-plane loading compared to walls reinforced with FRP. In the case of in-plane behaviour, the TRM technique results also in a positive effect on the resistance of about 65-70% compared with the FRP layers of identical configuration [11]. In terms of deformability, TRM was revealed to be more effective than FRP, but the efficiency varies greatly according to the type of wall and geometry (15-30% higher deformation in shear walls and up to 350% higher deformation in beam type walls) [9]. Furthermore, the strength generally increases with the number of layers and also depends greatly on the type of mortar [12-14]. Rupika (2010) [18] presented a work pointing out the performance of the different types of retrofitting on masonry infill walls. As reinforcing materials, steel meshes, glass fibre and polypropylene fibre mesh embedded in the mortar were considered. The steel mesh applied in plastering masonry walls subjected to bending tests revealed advantages in terms of maximum strength, although the observed deformation and ductility were not improved. The laminated polypropylene showed a low bearing capacity in relation to the other reinforcements but kept working after the opening of cracks led to high levels of deformation. The fibreglass meshes provided a high strength corresponding to the breakage of the fibres.

Bernat et al. (2013) [19] carried out a study based on the strengthening of masonry walls with the TRM technique with the purpose of understanding the influence of three different types of mortar, two different types of fibre (glass and carbon grids) and the possible benefit of using anchors to improve the connection between the walls and the external reinforcement. For this, an experimental campaign on real-size TRM strengthened masonry walls under eccentric compressive loads was carried out. It was observed that all the mortars reached the necessary bond strength to assure the adherence of the TRM to the masonry, so that no connectors

seemed necessary in the strengthening of walls under eccentric compressive loads. Indeed, the application of TRM has provided an increase of over 100% of the initial load-bearing capacity under eccentric axial load. Moreover, a stiffer and more homogeneous behaviour is noticed when TRM is applied. The in-plane stiffness has proved to be highly dependent on the type of strengthening mortar, whereas the out-of-plane stiffness is mainly defined by the type and amount of fibres.

Another aspect investigated was the technique of application of mortar (TRM), namely manually and sprayed mortar (TRSM) [20]. Different mortars and fibre grids achieved by using both types of application techniques were analysed. It was possible to conclude that there was a notable increase in productivity (between 2 and 6 times more) with TRSM, and it was also possible to obtain an enhanced resistance. Moreover, greater ductility values were also observed when TRSM is used in comparison with the TRM (same grid and mortar).

With respect to analytical modelling of composite materials used in the strengthening, namely layered materials and fibre reinforced material, homogenization techniques can be used to derive the mechanical properties [21-22]. In this respect, it is important to mention that the accurate prediction of macroscopic material properties of such materials on the basis of their microscopic mechanical behaviour is crucial for an efficient utilization of composite materials to engineering structures [21]. **Additional theoretical studies have been also carried out in the definition of analytical solutions for functionally graded materials, which can be applied to composite structures [23-28].**

Following the use of textile reinforcement mortar (TRM) as a retrofitting technique for masonry infill walls, some new textile fibre based materials manufactured through braiding techniques have been developed in the last years at the University of Minho, as an alternative to conventional FRP rods [8,11, 29-30]. This material, called braided composite rods (BCR),

which can be assembled as strengthening meshes, has some advantages such as the possibility of designing the composition according to mechanical requirements, the low manufacturing technology and the low-cost production. Moreover, the shape of the external surface can be optimized to improve the bond strength. Therefore, the main purpose of this paper is to provide the results on the mechanical performance of this novel material on the strengthening of brick masonry walls. For this, a detailed description of the strengthening, the manufacturing process and the results on the optimization of the surface of the rods based on tensile bond strength tests are provided. Additionally, the experimental campaign carried out on the evaluation of the performance of the braided rod meshes in the strengthening of brick masonry under flexure is presented and the main results are discussed. The performance of these meshes is also compared with the performance of different commercial meshes available in the market.

2. Description and mechanical characterization of braided composite rods (BCRs)

The strengthening material is designated as braided composite rod (BCR) and it results from a braiding process. This technique used for producing braided structures can be used for the manufacturing of fibrous reinforcements for construction applications [30] [20]. It has been used for two decades and it is being increasingly used for technical applications. The braided structure consists of a combination of three types of materials, each one with different functions. The braiding technique involves the braiding of yarns in the transverse and longitudinal directions, forming a tubular structure. These yarns are in two groups of spindles and rotate in opposite directions, clockwise and counter-clockwise [30]. With the aim of improving the mechanical properties and for adding new functionalities, axial fibres are added in the core of the rod (see Fig. 1a). The yarns that make up the base of the braid then involve a central core composed of reinforcing fibres that are responsible for the mechanical

performance. In Fig. 1b the representative scheme of the original transversal section of a BCR can be observed, having 16 multifilaments of polyester and a core filled with multifilaments of reinforcing fibres. In order to fill the voids between the materials and to give stability and homogeneity to the composite, a resin matrix is applied.

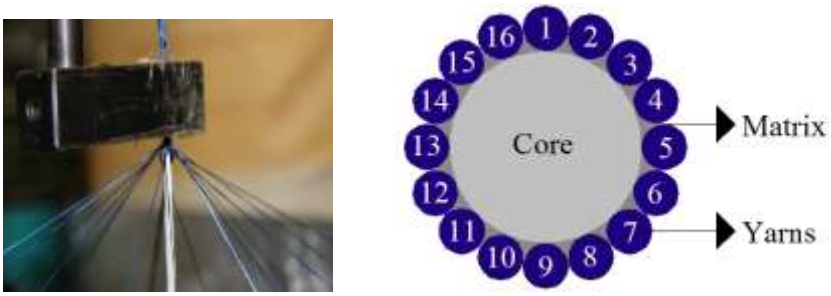

(a) (b)

Fig. 1 – Details of the braiding manufacture: (a) production; (b) schematic representation of the simple rod without roughness

The performance of the composite material depends largely on the effectiveness of the core, because it is intended that the loads are mostly absorbed by the reinforcing materials. It is necessary that the reinforcing material applied is chemically stable and has appropriate characteristics in terms of both tensile strength and density.

The composite braided rods are characterized by the braiding angle, which is the angle between the longitudinal axis and the direction of insertion of the braiding yarns, as can be seen in Fig. 2. The braiding angle is the most important parameter characterizing the textile braided structure, as it directly influences its mechanical behaviour [9, 29]. The diameter of the braid is the straight line connecting the two extremities passing through the braiding centre (see Fig. 2). This measure can vary according to the braiding yarn diameter, the diameter of the axial structure and circulation velocity [9, 29] .

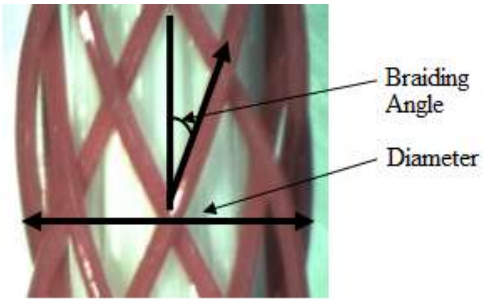

Fig. 2 – Braiding angle and diameter of BCR

The tensile behaviour of the braided composite rods can be obtained through uniaxial tensile tests based on NP EN ISO 2062 [31] and ASTM 5034 [32]. For the composite rod under study, which is intended to be used in the flexural strengthening of brick masonry walls, it was decided to use carbon and glass fibres for the core. The typical tensile behaviour of braided rods composed of different types of fibres is shown in Fig. 3. It is possible to observe the difference in the pre-peak regime and the similar behaviour after the peak load and failure of fibres of the core. After this failure, the external braid of polyester is totally loaded, which explains the existence of a long plateau after the peak resistance due to the high elasticity of the polyester braided rod.

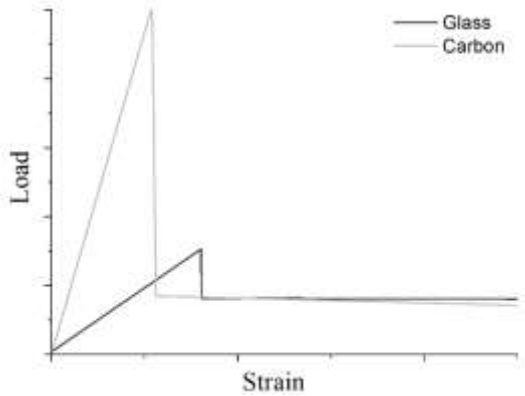

Fig. 3 - Typical tensile behaviour of the composite rods with glass and carbon fibres in the core

From the results of the uniaxial tensile tests, it is possible to conclude that the core reinforcement is responsible for the BCR's initial stiffness and resistance. Due to this, the

initial stiffness and maximum force of the carbon rods is higher than the stiffness of glass rods, as expected.

3. Optimization of the external braided roughness

3.1. Bond tests on individual rods

The composite rods can be composed of different materials and different configurations of yarns can be selected, leading to different roughness of the external surface to achieve optimized mechanical behaviour in terms of adhesion to mortar. Studies in terms of the adherence of the polyester rod to mortar were carried out by considering different structures for the braid. In total, 14 types of braid structure were selected (Table 1). Besides the simple braided rods (0bmin and 0bmax, produced at minimum and maximum speeds respectively), additional structures were considered by adding 1 or 2 multifilaments of 8 and 16 polyester yarns and by varying the production speed with specified minimum, maximum and intermediate values. As an example, the composite rod named 1b8min means that 1 multifilament of 8 polyester yarns was added and it was manufactured at the minimum specified speed. The schematic representation of the braided rods and cross-section with the indication of the resulting external roughness is given in Fig. 4. It is observed that either the additional multifilaments or the manufacture speed influences considerably the external roughness of the composite rods. From the representation it is also possible to observe that the introduction of two additional multifilaments leads to more obvious roughness and that the increase in the speed results in a more spaced roughness.

For each type of structure of the braided rods, 5 adherence tests (pull-out tests) were carried out, aiming at achieving a better insight into the bond behaviour of the distinct types of rods. Cylindrical specimens of mortar (5 mm diameter and 10 mm height) were cast, the rods being introduced at the centre through the total height of the cylinder (bond length of 100 mm).

Two types of mortar were used to evaluate also the influence of the strength of mortar on the bond behaviour. The mortar used in the second series of tests presented an average compressive strength of 3.56 MPa, representing an increase of about 77% in relation to the mortar used in the first series of tests (average strength of 2.01 MPa). The specimens were kept in laboratory conditions for 28 days. In the tip of the rod, an improved bond region was created, allowing its connection and fastening to the machine that pulls the rod out from the specimens of mortar (Fig. 5a). The procedure used for the pull-out tests was similar to that followed by other authors [29, 33-35].

Table 1 - Description of the braided structures

Sample Designation	Description of the samples	Speed (m/min)
0bmin	**1** to **16** multifilament polyester with 11 Tex	0.54
0bmax		1.07
1b8max	**1**- Braided multifilament consisting of 8 polyester 11 Tex **2 to 16**- multifilament polyester with 11 Tex	1.07
1b8int		0.8
1b8min		0.54
2b8max	**1 and 9 -** Braided multifilament consisting of 8 polyester 11 Tex **2 to 8 and 10 to 16 -** multifilament polyester with 11 Tex	1.07
2b8int		0.8
2b8min		0.54
1b16max	**1** - Braided multifilament consisting of 16 polyester 11 Tex **2 to 16**- multifilament polyester with 11 Tex	1.07
1b16int		0.8
1b16min		0.54
2b16max	**1 and 9 -** Braided multifilament consisting of 16 polyester 11 Tex **2 to 8 and 10 to 16 -** multifilament polyester with 11 Tex	1.07
2b16int		0.8
2b16min		0.54

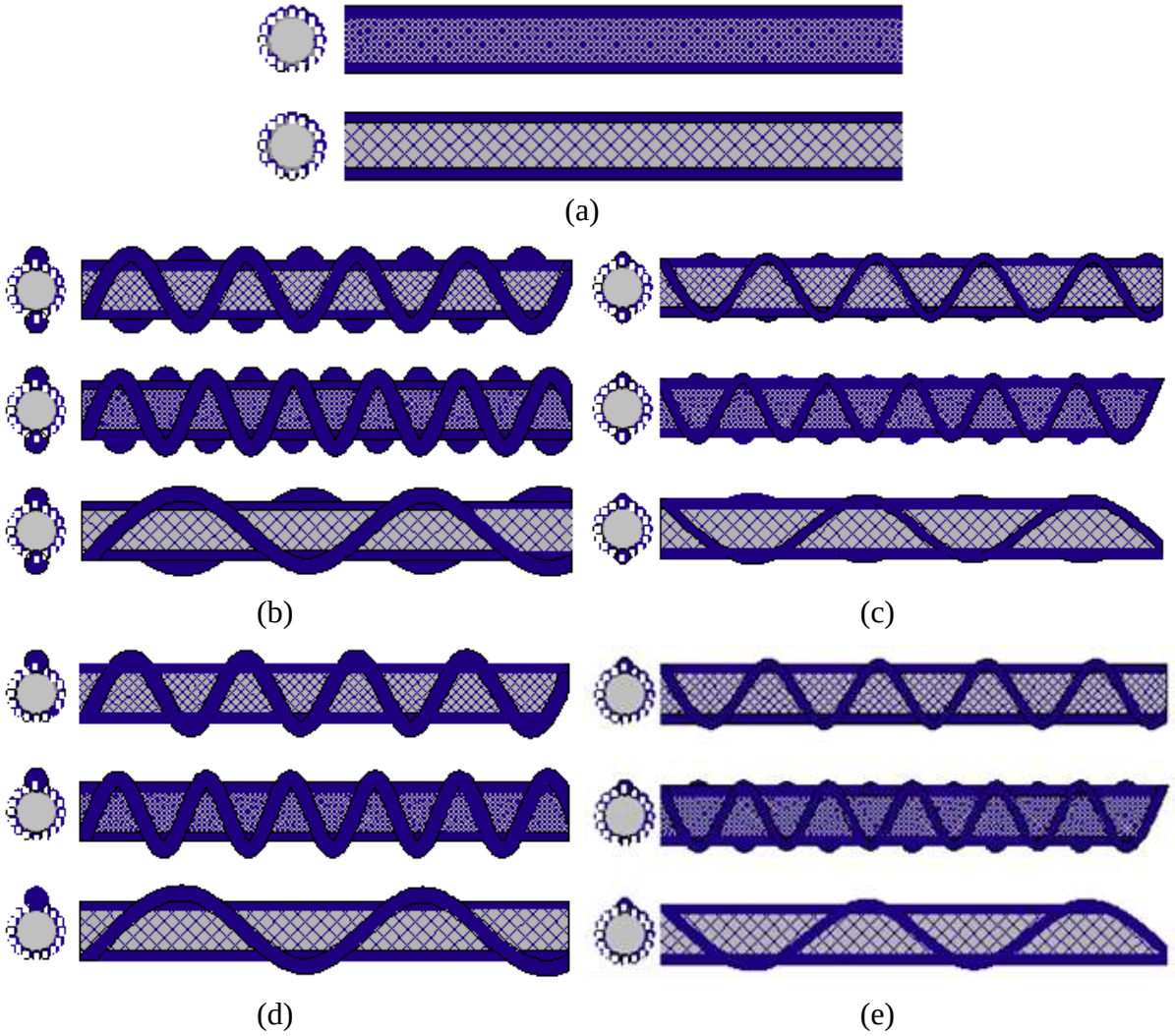

Fig. 4 – Schematic representation of the roughness of the composite rods: (a) without additional multifilaments (basic rods); (b) with additional 2 multifilaments with 16 polyester yarns (2b16int, min, max); (c) with additional 2 multifilaments with 8 polyester yarns (2b8int, min, max); (d) with additional 1 multifilament with 16 polyester yarns (1b16int, min, max); (e) with additional 1 multifilament with 8 polyester yarns (1b8int, min, max)

The pull-out tests were carried out on a stiff steel frame associated with a control system and a data acquisition system linked to a computer that allows the recording of the important information from the tests, namely loads and displacements. The vertical tensile load was applied through a hydraulic actuator and measured through a load cell with a maximum

capacity of 10 kN, and the linear sliding of the rod was measured by means of an LVDT (Linear Variable Differential Transducer) attached to it.

The cylindrical specimens of mortar were confined vertically through the use of two steel plates previously levelled and connected together, in order to prevent any axial deformation of the mortar specimens and to promote the relative displacement between the rod and the mortar specimens (Fig. 5b). The test was carried out under displacement control at a rate of 0.010 mm/s, which corresponds to a test duration of approximately 45 to 60 min.

(a) (b)

Fig. 5 – Details of the pull-out tests; (a) production of specimens; (b) test set-up

The load-sliding diagrams obtained for the pull-out tests for the distinct structures of the braided rods are presented in Fig. 6. These diagrams are characterized by a sharp load increase in the pre-peak regime, which is associated with a high initial stiffness. After the peak load is attained, a progressive decrease in the bearing load is accompanied by an increase in the sliding of the rods from the concrete cylinder. A steeper post-peak branch was found for the mortar with higher strength. It is clear that the adherence is considerably lower in the case of the standard braided rods, without roughness (0bmin). The average bond strength obtained for each roughness and for each test series is presented in Fig. 7. In spite of the scatter found in the results, it is possible to observe that the roughness formed by a simple

braid with 8 yarns exhibited a more satisfactory behaviour than the roughness with 16 yarns, in terms of both bond strength and deformation capacity.

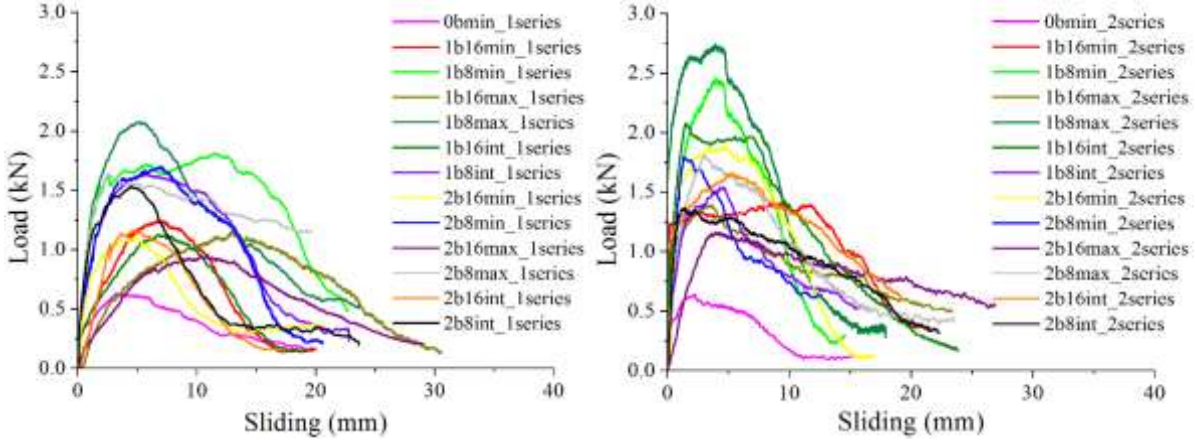

(a) **(b)**

Fig. 6 – Force-sliding diagrams obtained in the pull-out tests: (a) series 1; (b) series 2

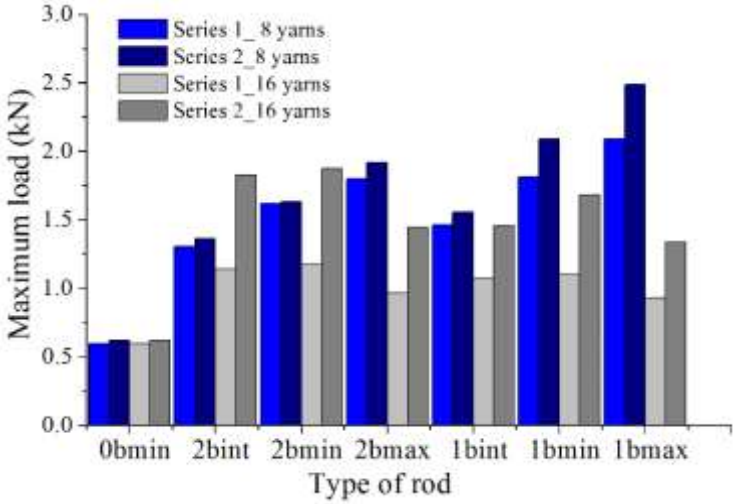

Fig. 7 - Maximum bond load for each type of rod

It appears that the bond strength depends on the interaction of the roughness with the surrounding mortar (Fig. 8). Both the increase in the spacing of the salient roughness and the interlocking controlled by the roughness result in a better bond adherence. This should be attributed to the better involvement of the braided composite by the mortar. It is possible that the minimum spacing of the salient roughness promotes deficient filling of the mortar and, thus, the decrease in the interlocking.

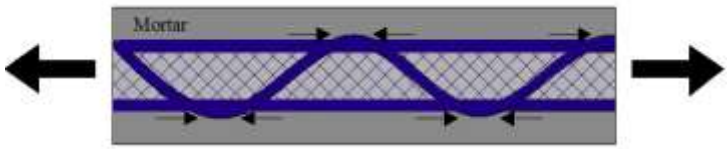

Fig. 8 – Schematic representation of interlocking controlled by roughness

It is also observed that the mortar strength has an influence on the bond behaviour of the braided rods, leading to higher values of bond strength when its strength is higher. Lower values of mortar strength result also in more ductile post-peak behaviour.

To sum up, it should be stressed that the most satisfactory performance in terms of maximum force recorded was found for the braided rod with the structure designated by 1b8max (braided rod with one additional multifilament composed of 8 yarns of polyester manufactured with the maximum braiding velocity). Nevertheless, during the manufacturing process it was found to be impossible to produce this structure for the reinforcing mesh to be applied in the masonry specimens due to the lack of homogeneity of the finished braid, since it was necessary to increase the amount of material in the core so that a mesh comparable to the commercial ones could be attained. It could also be concluded that the manufacture of the rods from the braiding technique with specific conditions may depend on the diameter of the reinforcement to be included in the core. Therefore, the alternative braided structure selected for the rod to be applied in the reinforcing meshes was 1b8min, consisting of 15 multifilament polyester 11 Tex and 1 element of braided simple structure consisting of 8 braided polyester yarns produced with the minimum speed of the production equipment (0.54 m/min). With this manufacturing rate, the braid protects the core totally because the minimum speed allows better involvement of the core (see Fig. 9).

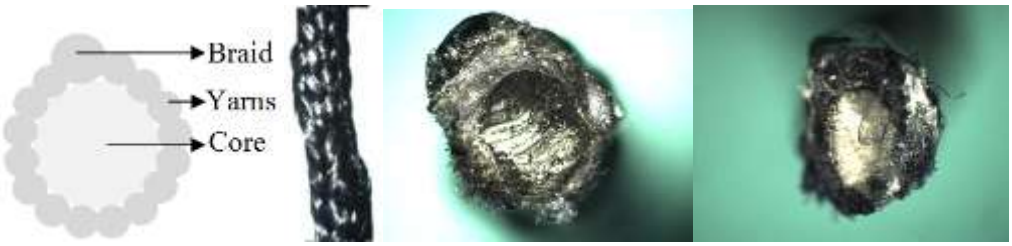

(a) (b) (c) (d)

Fig. 9 – Details of the composite braided rods used in the manufactured meshes: (a) representation of the cross-section of a BCR 1b8min; (b) front view of the braided 1b8min; (c) cross-section of the BCR used in carbon mesh; (d) cross-section of the BCR used in glass mesh

3.2. Bond tests on meshes of BCRs

Reinforcing meshes were developed with the selected braided structure in order to understand the behaviour of a set of rods when pulled out inside the plaster mortar, as happens in strengthened masonry under flexural loading. The core of the rods used in the pull-out tests is composed of two multifilaments of carbon 1600 Tex with the selected braided structure 1b8min, and are intended to be applied in reinforcing meshes of masonry walls. Besides this braided structure, the original configuration without roughness (0bmin) was also produced in order to analyse the influence of the roughness on the bond strength. The manufacturing of the meshes is done by interlacing the rods in two directions. The configuration of the connections of rods leads to some waviness of the mesh, which can result in additional imbrication (Fig. 10).

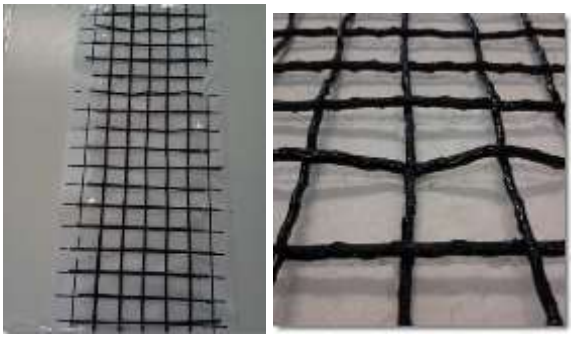

Fig. 10 – View of the reinforcing mesh

Besides the study of the meshes composed of the braided composite rods, two commercial solutions with similar mechanical and physical characteristics were tested in order to compare their behaviour with that of the manufactured meshes. The commercial meshes are different in terms of type of fibres, one of them being composed of carbon fibres in the main direction (Comm_carb) and the other one composed of glass fibres in two perpendicular directions (Comm_glass). The commercial mesh with carbon fibres (Comm_carb) is unidirectional, taking into account that carbon fibres are oriented in the direction where bending develops, and has a density of 200 g/m and a spacing of approximately 25 mm in the main direction. Based on the technical information, the mesh has a flexural strength of 93.6 kN/m and presents an extension at maximum stress of 1.75 %. The commercial mesh of glass fibres (Comm_glass) consists of resistant glass fibres in both directions. Once bidirectional, the mesh density is 225 g/m^2 with spacing between the fibres of 25 mm. From the technical information, it is seen that the flexural strength is 45 kN/m with associated extension at peak stress less than or equal to 3%. Because the commercial meshes present a spacing of 25 mm, the manufactured meshes were manufactured with the same spacing.

The construction of representative masonry specimens to which the reinforcing meshes were applied was done by an experienced mason in order to reproduce workmanship similar to that used in current practice. A mortar layer was applied on a brick unit in which the reinforcing meshes were embedded (see Fig. 12). The area of mesh embedded in the rendering mortar was about 200 mm x 100 mm (length x width), equal to the free area to enable its adequate connection to the testing machine. On the tip of each mesh, a stronger bond in the individual rods was prepared, aiming at strengthening the connection and fastening of the mesh to the grip of the testing machine. For each typology of mesh, 5 tests

were considered taking into account the possible scatter in the results. The thickness of mortar (20 mm) is the same as the masonry specimens to be built for the flexural tests. The mortar used in the construction of the specimens was the mortar with the highest compressive strength used in the bond tests of the braided rods. The samples were kept under relatively stable conditions of temperature and humidity inside the laboratory.

(a) (b)

Fig. 11 – Commercial meshes used in the pull-out tests: (a) comm_carb; (b) comm_glass

Fig. 12 – Application of meshes on masonry bricks

The test set-up for the bond tests on the meshes was based on the testing configuration used for the bond tests of individual rods (see Fig. 13). The brick unit was confined with two steel plates so that the mesh could be pulled out from the mortar layer of the masonry unit. The tensile load was applied through a hydraulic actuator and measured by a load cell with a maximum capacity of 200 kN. The tests were carried out under displacement control at a rate of 0.08 mm/s. The deformation was measured by the internal transducer of the machine.

Fig. 13 – Test set-up used in the bond tests of strengthening meshes

The typical load-sliding diagrams found in the bond tests are displayed in Fig. 14. In all cases no sliding of the rods from the grip test was recorded, the tests thus being considered valid. It was observed that the behaviour of specimens with the mesh with 1b8min rods presented very similar behaviour to the commercial mesh composed of carbon fibres. The maximum force was almost the same, and the post-peak was also similar. After an abrupt reduction of the load-bearing capacity just after the peak load was reached, both meshes were able to bear decreasing load with increasing displacements. In both meshes very major ultimate displacements could be found, corresponding practically to the collapse of the bond. The mesh composed of rods without roughness presented a fragile behaviour. Although these meshes also presented a transverse and longitudinal interlacing of rods and had the same geometrical characteristics and shape as the mesh with the 1b8min rods, the interlocking is more relevant for the latter mesh due to the additional roughness of each rod. This additional roughness acts as a friction agent, promoting enhanced adhesion. On the other hand, the commercial mesh with glass fibres presented a very fragile behaviour, which was associated with the premature breakage of the glass fibres before these had been pulled out from the mortar.

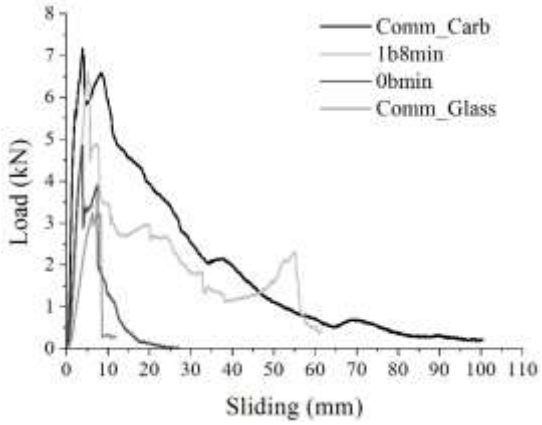

Fig. 14 – Typical load-sliding diagrams of the meshes

The cracking pattern of the manufactured meshes presented the formation of multiple cracks associated with the re-distribution of forces, together with the fragmentation and detachment of the mortar in the plastering in some cases (Fig. 15). The commercial mesh with carbon fibres showed only one crack, through which the mesh slid when it was pulled out (Fig. 15). This difference can be associated also with the higher interlocking that the manufactured meshes develop due the interlacing of rods, an aspect that is not visible in the very flat commercial mesh.

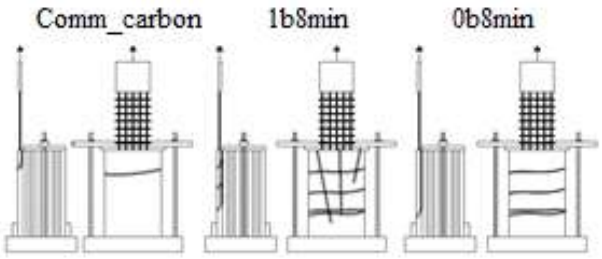

Fig. 15 – Cracking patterns observed in the pull-out tests of the meshes

4. Strengthening of masonry under flexure

In order to assess the mechanical performance of the proposed strengthening meshes composed of braided composite rods in the improvement of brick masonry walls under out-of-plane loading, an experimental campaign based on flexural tests was carried out on

masonry walls. The brick masonry is intended to represent the typical masonry infills used in the reinforced concrete frames that are widely used as a constructive system in Portugal and other countries, particularly in southern Europe.

4.1. Materials

The masonry walls are composed of brick units with horizontal perforations of the kind mostly used in the construction of masonry infill walls in Portugal, with dimensions of 300 mm x 200 mm x 150 mm (length x height x thickness). Four bricks were tested under uniaxial compression according to EN 772-1 [36] in the direction of the horizontal perforations. Although the compressive strength normal to bed joints is commonly required, in the case of out-of-plane flexure in the parallel direction to the bed joints (cracking developing in the perpendicular direction to the bed joints), the compressive strength of masonry in the parallel direction to the bed joints is required. The average compressive strength of the brick units obtained was 4.5 MPa. Taking into consideration the correction factor δ of 1.35 based on the dimensions of the brick and of the loading configuration, the normalized compressive strength of the brick units is 6.1 MPa.

The laying of the bricks was carried out with general purpose mortar M10, whereas for the finishing a commonly used rendering mortar was used. In order to control the quality of the mortar, three specimens with dimensions 40 mm x 40 mm x 160 mm, taken during the construction of the specimens, were tested in bending and compression after 28 days according to EN 1015-11 (1999) [37]. The average compressive strength of the mortar was about 7.2 MPa, whereas the flexural strength was 2.4 MPa with a coefficient of variation of 5% in both cases. For the rendering mortar, an average compressive strength of 3.87 MPa (coefficient of variation of 21.3%) and an average bending strength of 1.02 MPa (coefficient of variation of 20.1%) were obtained.

Taking into account the results obtained in the individual bond tests and as already mentioned, the 1b8min structure was selected for the manufacture of the BCR mesh. To have manufactured meshes that are comparable with commercial meshes (see section 3.1.2), 3 carbon multifilaments of 1600 Tex were required, corresponding to a density of 182 g/m (about 91% compared to commercial mesh comm_carb), and 5 glass multifilaments of the 544 Tex were required, corresponding to a density of 207 g/m^2 (about 92% compared to commercial mesh comm_glass mesh). Manufacturing of the meshes is carried out by interlacing the composite rods in two directions, assuming that the configuration of the connections of rods in the two directions may promote an additional interlocking and can work as an additional roughness, improving the bond adherence between the meshes and the rendering mortar (Fig. 16).

Fig. 16 - Detail of the manufactured carbon mesh

4.2. Masonry specimens

The number and description of the specimens used in the experimental campaign of flexural tests on brick masonry is presented in Table 2. A reference masonry specimen is considered to assess the performance of the strengthened specimens in terms of both load capacity and ultimate deformation. The manufactured meshes are also compared with the two commercial meshes based on carbon (unidirectional mesh) and glass fibres (bidirectional mesh).

Table 2 - Typology and number of specimens tested to out-of-plane flexure

Sample Code	Sample Description	Number
Reference	Masonry wall without reinforcement	3
Comm_carb	Masonry wall with commercial mesh comm_carb	3
Comm_glass	Masonry wall with commercial mesh comm_glass	3
Mesh_carbon	Masonry wall with a BCR mesh with a reinforcing core composed of 3 yarns of carbon and a braided structure of type 1b8min	3
Mesh_glass	Masonry wall with a BCR mesh with a reinforcing core composed of 5 yarns of glass and a braided structure of type 1b8min	3

The geometry of the masonry specimens and in particular the definition of the length to thickness ratio is based on the work performed by Gómez (2012), Papanicolaou et al. (2007), Rupika (2010) and Abreu (2011) [8,13,18, 38], and based on EN-1052-2-99 [39]. It was decided to consider the flexure parallel to the bed joints, taking into account that during the construction of the masonry infill walls, the top bed joint is often not adequately filled, resulting in the separation of the top border and leading to the development of bending in the direction parallel to the bed joints. A length to thickness ratio of approximately 10 was adopted. On the other hand, the dimensions adopted for the masonry specimens fully comply with the recommendations of the European standard (see Fig. 17). Regarding the configuration of the load application, a four-point bending load configuration was adopted. The supports are spaced about 50 mm from the border of the specimen, whereas the load application points are spaced about 350 mm, the distance from the support being about 525 mm.

The construction of the masonry specimens was done by an experienced mason in order to have similar workmanship to that used in current structures. The samples were kept under relatively stable environment conditions of temperature and humidity inside the laboratory. The rendering of the specimens with the introduction of the strengthening meshes was done two weeks after the construction of the specimens. This was done by applying a thin layer of mortar, with subsequent placement of the reinforcing mesh embedded in a new layer of

rendering mortar, giving a total thickness of about 20 mm. Moreover, even in the unreinforced masonry walls the rendering was applied with a thickness of 20 mm for better comparison of results (Fig. 18). Note that the reinforced plaster was applied only on one side of the specimen because it is assumed that in real applications only one surface of the cavity enclosure wall is accessible for application of the reinforcement. Another aspect is the application of the mesh to the entire length of the wall.

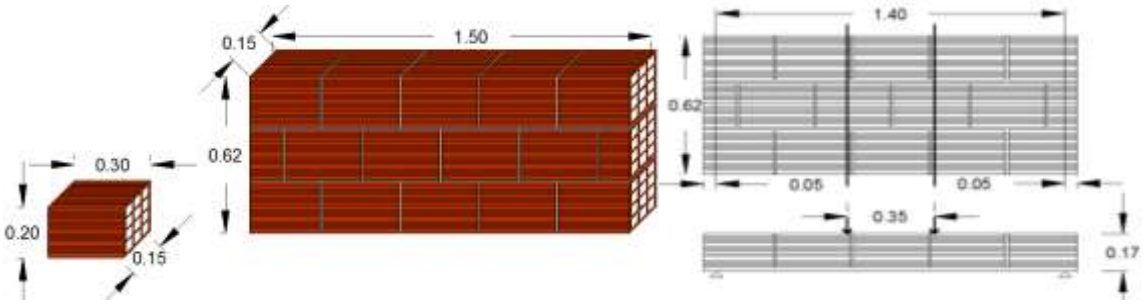

Fig. 17 - Geometry of the specimens and load configuration (dimensions in meters)

Fig. 18 - Construction of the walls and application of reinforcement mesh

4.3. Test set-up

As already mentioned, the four point loading configuration was adopted for the flexural tests in specimens with a free span of 1400 mm (Fig. 19a). The test set-up consists of a steel frame attached to a reaction slab with a vertical jack (capacity of 500 kN) connected to a load cell to

measure the applied load with a capacity of 200 kN. For the unreinforced walls, only monotonic loading was applied. In the strengthened specimens, both monotonic and cyclic loading was considered in order to understand the effect of the cyclic loading in the mechanical behaviour of strengthened masonry. Regarding the monotonic test, this was developed in three stages according to the phenomena observed when the load applied is controlled by an external displacement: (1) the first step corresponds to a speed of 0.004 mm/s up to the cracking of the specimens; (2) the second step is performed at a speed of 0.01 mm/s up to the vicinity of the peak load; (3) the third and last step, a speed of 0.02 mm/s, was considered so that a reasonable total duration of the test is achieved due to the high deformation level developed.

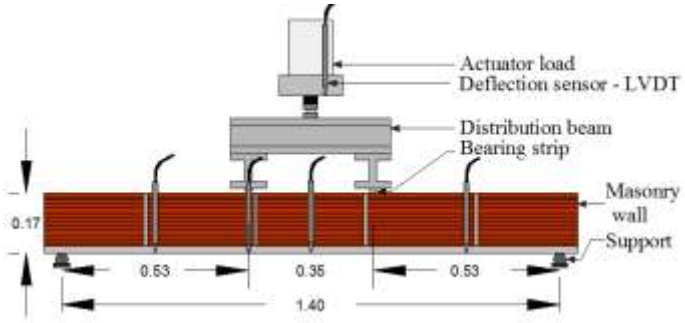

(a)

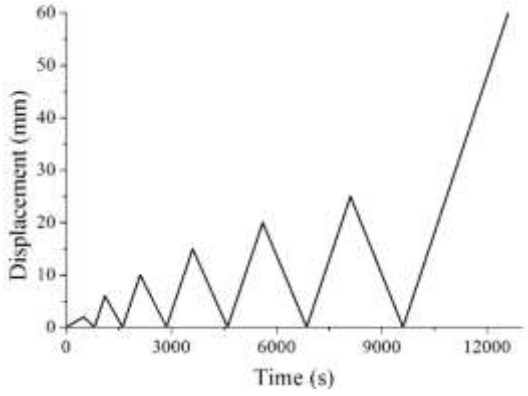

(b)

Fig. 19 - Experimental details: (a) test set-up (dimensions in meters); (b) displacement-time history

With respect to measurement devices, the deformation of the samples was measured using four linear voltage displacement transducers (LVDTs): one LVDT at the mid span, to record the highest deformation of the specimen, two LVDTs between the supports and the points of load application and one LVDT located in the loading direction. An LVDT was also attached to the actuator and used as external control (Fig. 19a). For the application of the load, a structure with I-shaped steel profiles was used. The simple supports were metal rods to which an elastic material between the rod and the sample was added to prevent friction between the two surfaces. In the cyclic test a displacement-time history was adopted according to the diagram shown in Fig.19b in order to understand the cyclic behaviour under flexure.

5. Analysis of results

To analyse the results of the bending tests, distinct data were considered, namely: (1) force-displacement diagrams; (2) damage patterns, and (3) complementary quantitative parameters aimed at better understanding the flexural behaviour of the strengthened masonry specimens.

5.1. Force-displacement diagrams

The flexural behaviour of the brick masonry was evaluated in a first stage by means of the force-displacement diagrams, which provide information about the maximum resistance, deformation at peak load, and ultimate deformation capacity of the masonry. The force-displacement diagrams obtained for all specimens are presented in Fig. 20. From the force-displacement diagrams some key parameters were defined in order to better analyse and compare the different strengthening solutions, namely the load corresponding to the first cracking, f_{cr}, and corresponding displacement, δ_{cr}, the maximum load, f_{max}, and the corresponding displacement, δ_{max}, and the relation between the cracked stiffness, k_1, (stiffness after the appearance of the first flexural cracks) and the initial stiffness, k_0, corresponding to

linear stiffness (until the onset of the first flexural crack), (k_1/k_0). The average values are summarized in Table 3.

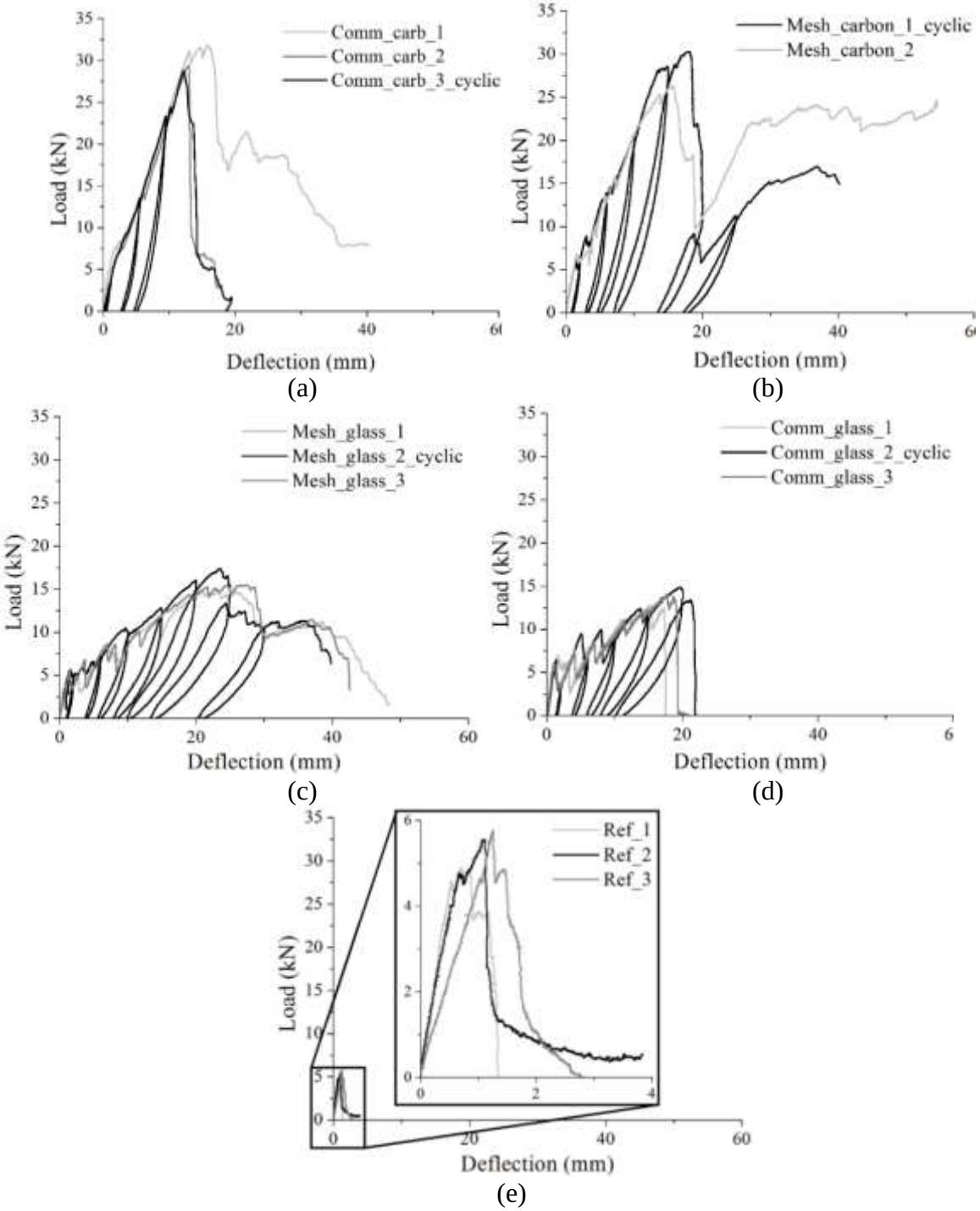

Fig. 20 - Load-deflection response of the masonry samples: (a) with BCR carbon mesh; (b) with comm_carb mesh; (c) with BCR glass mesh; (d) with comm_glass mesh; and (e) unreinforced

Table 3 – Average values of key parameters derived from force-displacement diagrams

Type	f_{cr} (kN)	δ_{cr} (mm)	f_{max} (kN)	δ_{max} (mm)	K_1/K_0 (%)
Reference	4.55	0.73	5.41	1.01	-
Comm_carb	5.58	1.39	28.20	12.78	48.57
Δ ref. (%)	122.5	190.35	521.13	1266.4	-
Mesh_ carbon	6.11	2.00	29.44	16.99	40.20
Δ ref. (%)	134.2	273.71	544.09	1683.0	-
Comm_glass	5.56	1.03	12.27	13.68	8.86
Δ ref. (%)	122.2	141.56	226.74	1355.7	-
Mesh_glass	4.89	1.20	15.85	25.67	10.55
Δ ref. (%)	107.4	164.84	292.96	2543.1	-

It is observed that unreinforced specimens present very fragile behaviour, which is associated with much localized cracking involving the failure of the unit-mortar interfaces and units.

On the other hand, the brick masonry presents very stiff behaviour in the pre-peak regime with very low displacement until the peak load is attained. The flexural behaviour of specimens reinforced with FRP-based meshes is characterized by a very stiff pre-peak behaviour, the pre-peak branch having two distinct slopes (almost a pre-peak bilinear branch): (1) the first slope associated with the linear elastic behaviour of the specimens (k_0); (2) the second slope corresponding to the cracked state of the masonry until the peak load (k_1). For the specimens reinforced with glass fibre meshes, the decrease in the slope of the second branch is higher than in the case of specimens strengthened with meshes with carbon fibres, which is associated with lower cracked stiffness of the specimens. This behaviour is reflected by the considerably lower values of the ratio between the linear and cracked stiffness (k_1/k_0) (see Table 4). The deflection corresponding to the peak load is then higher in the case of the specimens reinforced with glass fibre meshes. The manufactured meshes with glass fibres present a very reasonable post-peak behaviour, with the progressive reduction of strength with increasing displacements. The ultimate deflections are about 40 mm, considerably higher than

the ultimate deformation obtained in the specimens reinforced with the commercial glass fibre meshes. Instead, these specimens present a very fragile behaviour and the peak load stage corresponds to the abrupt failure of the specimens.

The masonry strengthened with the manufactured meshes based on BRCs with carbon fibres presents more nonlinearity in the pre-peak regime than in the case of specimens strengthened with commercial meshes. The post-peak behaviour is similar just after the attainment of the maximum load, but in the case of commercial meshes, the specimens present a very steep descending branch and no recovery of loading was visible. On the contrary, if manufactured meshes are used, the specimens are able to recover the resistance after the decrease in the bearing capacity just after attaining the peak load (Fig. 20a,b).

It is seen that the strengthening of the brick masonry results in an increase in the flexural cracking load with respect to the unreinforced masonry, the increase being of 25% and 34% for the commercial and manufactured carbon fibre meshes respectively, and of 22% and 7% for the commercial and manufactured glass fibre meshes respectively. The displacement corresponding to the cracking load increases also with the strengthening of the masonry. As expected, the maximum flexural load increases considerably when strengthening meshes are applied in the brick masonry specimens. It is observed that the increase in the flexural strength is about 5.2 times that in specimens strengthened with commercial carbon fibre meshes and about 5.4 times that in the case of manufactured carbon fibre meshes. In the case of brick masonry specimens strengthened with glass fibre meshes, the flexural strength is 2.3 times higher in the case of commercial meshes and 2.9 times higher in the case of manufactured meshes. These results show that the carbon meshes are more efficient in the enhancement of the flexural strength of brick masonry than the meshes with glass fibres. On the other hand, the manufactured meshes with BCRs perform better than the commercial

meshes, particularly in the case of meshes with glass fibres. This becomes more significant if the percentage of reinforcement in the manufactured meshes is compared to the commercial ones, as in both cases the percentage of reinforcement is approximately 91% of the reinforcement existing in the commercial meshes.

The improvement in the deformation capacity of the strengthened masonry is clear when the maximum displacements are analysed. The ultimate displacement increases by 12.7 times and 16.8 times in the case of application of commercial and manufactured carbon fibre meshes respectively. The use of the commercial mesh with glass fibres results in an increase in the ultimate displacement of 13.6 times in the unreinforced specimens, while the use of the manufactured mesh with glass fibres results in an ultimate displacement of 25.4 times the reference ultimate displacement. With respect to the deformation ability, it is observed that the manufactured meshes clearly perform better than the commercial meshes, and it is important to highlight the performance of the manufactured mesh with glass fibres. In addition, it should be noticed that the ultimate displacement obtained in the specimens strengthened with the commercial mesh with glass fibres corresponds practically to the displacement at the peak load, as the failure develops just after this stage. The higher capacity of the brick masonry strengthened with manufactured meshes to deform in the nonlinear regime should be attributed to the external structure of the BCR, composed of a polyester shell designed to ensure a substantial residual resistance and deformation ability after the maximum resistance and failure of the reinforcing core is attained.

In order to better analyse the cyclic behaviour of the masonry specimens, it was decided to evaluate the variation of the cyclic stiffness with flexural load and displacement. The stiffness is calculated by the slope of the line connecting the points of the cyclic loops. It is interesting to notice that the evolution of the stiffness degradation versus the flexural load and deflection

during the cyclic loading differs considerably if strengthening is carried out by means of meshes with carbon or glass fibres. In both types of fibre, the behaviour of the commercial and manufactured meshes is very similar. The flexural stiffness degradation vs. flexural load is described by a linear trend in the case of specimens strengthened with meshes based on carbon fibres. In the specimens reinforced with meshes with glass fibres present, the flexural stiffness degradation vs. flexural load is described by an exponential decreasing trend. This means that the cyclic stiffness degradation is more pronounced in the case of specimens with meshes with glass fibres than in meshes with carbon fibres. In any type of fibre, it is observed that the manufactured meshes present a better behaviour, and it is important to highlight the remarkable ability of the manufactured mesh with glass fibres to degrade stiffness until very high deflection values.

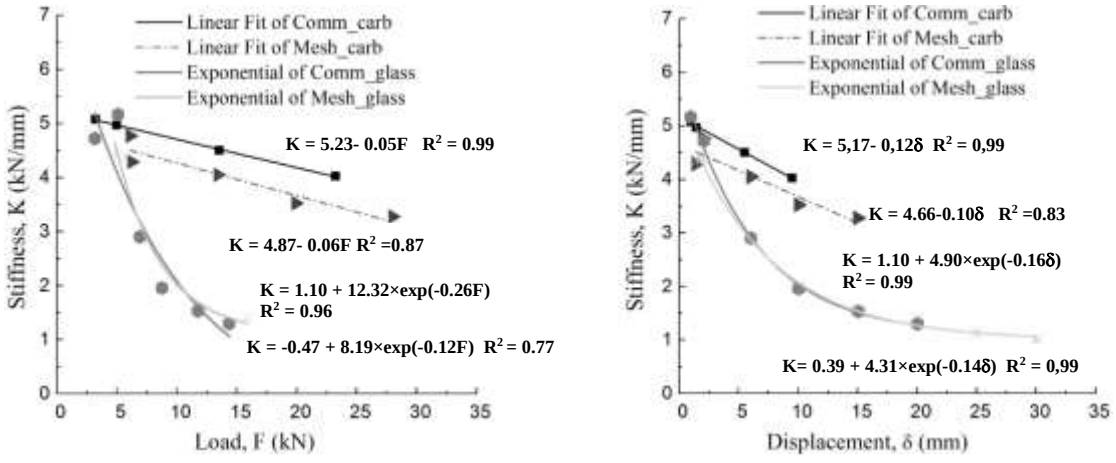

(a) (b)

Fig. 21 - Correlation between cyclic stiffness and: (a) load and (b) deflection

5.2. Crack patterns and failure modes

The walls without reinforcement exhibited a very brittle behaviour. The failure developed immediately after achievement of the maximum load, without displaying additional

deformation capacity. In the unreinforced specimens, a localized crack at the mid span of the specimen developed (Fig. 22).

Fig. 22 - Typical failure mode in unreinforced specimens

The brick masonry specimens strengthened with the commercial meshes show unexpected brittle behaviour compared to the specimens strengthened with manufactured meshes, which exhibited a much more ductile behaviour. The crack patterns of the strengthened specimens present multiple transversal cracks, resulting from the ability of the strengthening meshes to better distribute the flexural stresses (Fig. 23).

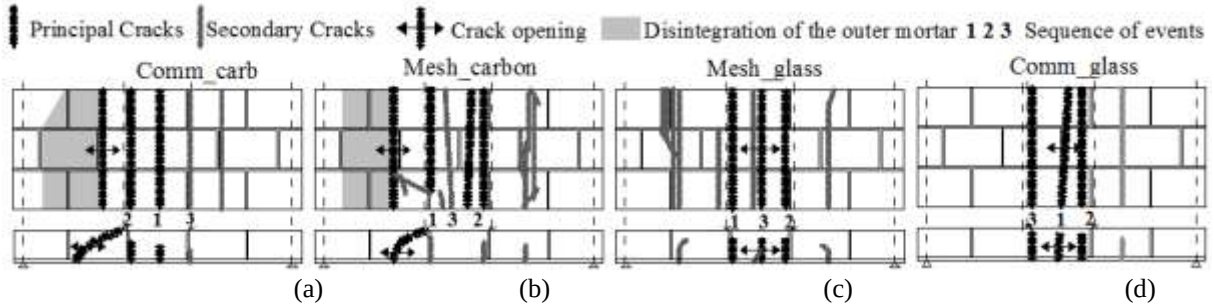

Fig. 23 – Typical cracking patterns observed in brick masonry specimens strengthened with: (a) commercial carb mesh; (b) manufactured carbon fibre mesh; (c) manufactured glass fibre mesh; (d) commercial glass mesh

It is clear in all cases that the principal cracks are due to tensile stresses associated with the bending of the specimens. These flexural cracks are responsible for the considerable reduction in the flexural stiffness, which decreases by 50% and 60% in the case of commercial and

manufactured carbon fibre meshes. The reduction of the initial stiffness is considerably more relevant in the case of the brick specimens reinforced with glass fibres, the plastic stiffness being around 10% of the initial stiffness (Table 4).

When the strengthening of the brick masonry is done with carbon meshes, shear cracks also develop in the vicinity of the supports (Fig. 24a,b), leading to the final collapse in a mixed shear and flexure mode. This behaviour is associated with the very high flexural strength that it is possible to attain with these meshes: the progressive increasing of the load and deformation results in the opening of shear cracks that somehow control the failure mechanism of the brick masonry.

(a)

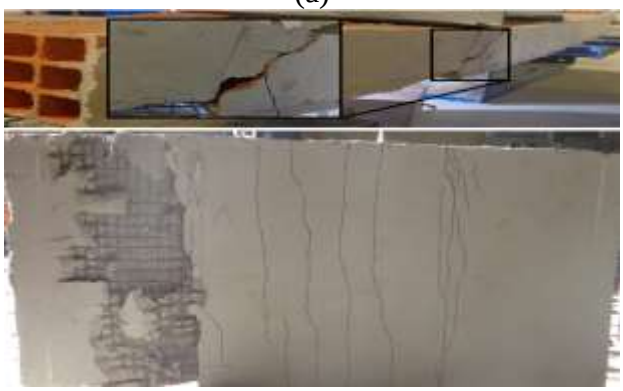

(b)

(c) (d)

Fig. 24 - Typical failure observed in brick masonry specimens strengthened with: (a) commercial carb mesh; (b) manufactured carbon mesh; (c) manufactured glass mesh; (d) commercial glass mesh

More brittle behaviour of brick masonry reinforced with carbon fibre meshes is observed, and particularly in the specimens strengthened with the commercial fibre mesh the response is controlled by shear for large deformations. It should be highlighted that, unlike the commercial carbon fibre mesh, the manufactured carbon fibre mesh provides high levels of deformation at very high levels of resistance (about 90% of maximum load), which results in a very ductile behaviour of the sample with a pattern of additional multiple micro-cracks. The difference in relation to the commercial carbon mesh is explained by the phased breakage of the carbon fibres in the reinforced core of the BCR at different levels of strain, enabling a high redistribution of forces and the formation of multiple cracks. Additionally, the presence of the external polyester ensures a residual bearing capacity for high levels of deformation. The superficial roughness of the polyester rod promotes an enhanced adherence, contributing also to the better performance.

The masonry specimens with meshes with glass fibres presented only flexural cracks and these are more concentrated in the length of pure flexure (Fig. 22c,d and Fig. 24c,d). In this respect, it is important to notice that a larger amount of cracks is observed in the specimens with manufactured meshes (Fig. 22). Contrarily to the specimens with carbon meshes, no shear cracks developed, meaning that these specimens collapsed by pure bending. Although the cracking patterns are very similar between the specimens reinforced with commercial and

manufactured meshes with glass fibres, the deformation ability is considerably higher in the case of manufactured meshes, it being possible to achieve very significant deformation without signs of collapse (Fig. 24c). Notice that the failure of the specimens reinforced with commercial meshes with glass fibres occurred just after achievement of the peak load (Fig. 24d). The better performance of the manufactured meshes with glass fibres can be explained also by the presence of the external polyester braided rods, which provides the deformation ability of the masonry with a reasonable residual resistance.

5.3. Indicative performance indexes

With the aim of evaluating the flexural performance of the strengthened masonry specimens, it was decided to assess the deformation capacity of the specimens in a quantitative way. For this, as an additional comparison of the deformation capacity of the reinforced walls, the ductility factors associated with deformation measured at the peak load (μ_{fmax}) and with the ultimate deformation (μ_{max}) were calculated according to equations (2) and (3) respectively:

$$\mu_{F_{max}} = \frac{\delta_{F_{max}}}{\delta_{cr}} \tag{2}$$

$$\mu_{max} = \frac{\delta_{max}}{\delta_{cr}} \tag{3}$$

where δ_{fmax} is the average displacement corresponding to the maximum force, δ_{max} is the average maximum displacement and δ_{cr} is the average displacement corresponding to cracking initiation.

The results obtained for the ductility factors shown in Fig. 25a confirm the better performance of the manufactured meshes in terms of deformation, it being possible to measure the ultimate ductility factor, which it is not possible to measure in the case of commercial meshes. On the other hand, it is possible to observe that higher deformation factors corresponding to the peak

load are obtained also for the manufactured meshes. These results also confirm the better performance of the manufactured mesh based on glass fibres in terms of deformation capacity. As expected, the unreinforced specimens present the lowest ductility factor corresponding to the peak load.

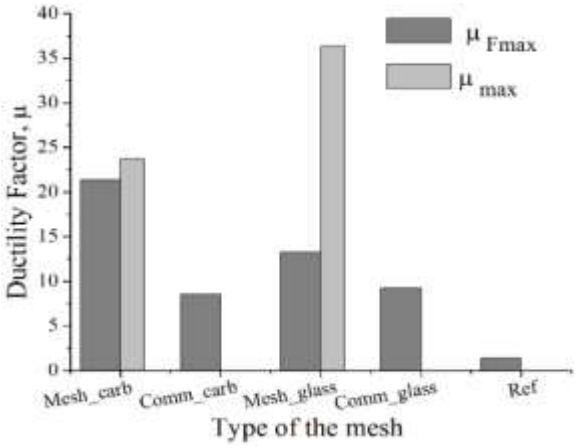

Fig. 25 – Values of the ductility factor for the different meshes

6. Conclusions

In this work, an innovative strengthening technique based on textile-reinforced mortar with strengthening meshes based on BCRs is presented and used in the strengthening of brick masonry under out-of-plane bending. A BCR is a composite rod composed of an external polyester protection of a reinforcing core composed of distinct types of fibres. The idea is that the core provides the reinforcement and the external polyester braided rod gives the residual strength and deformation capacity, controls the damage and avoids brittle failure of the brick masonry. Synthetic and natural fibres can be used in the reinforcing core.

An extended experimental campaign was designed based on: (1) the bond adherence of the composite rods to define the external structure of the polyester braided rods that resulted in the better adherence to the rendering mortar; (2) the bending tests of unreinforced and strengthened brick masonry with braided composite meshes and commercial meshes. In this experimental campaign, it was possible to compare manufactured meshes and commercial

meshes, which are approximately equivalent in terms of the amount of reinforcing fibres. With regard to the results of the experimental campaign on bond tests and to the out-of-plane bending tests carried out on brick masonry strengthened with distinct types of textile meshes, it can be concluded that:

1. The optimum typology of the braided structure to apply in the strengthening of masonry walls consists of 15 multifilaments of polyester with 11 Tex and 1 braided element with a simple structure consisting of 8 braided polyester yarns, produced at the maximum speed of the production equipment. The idea is that this structure presents an irregular external roughness that increases the bond adherence between the polyester rod and the rendering mortar.
2. The strengthening of the brick masonry results in an increase in the flexural cracking load. The increase ranges from 7% to 34% for the manufactured mesh with glass and carbon fibres respectively.
3. The flexural cracked stiffness of the strengthened brick masonry is considerably reduced when the meshes with glass fibres are used. The cracked stiffness is about 50% of the initial stiffness in the case of carbon fibre meshes and of 10% in the case of meshes with glass fibres.
4. The maximum resistance to bending is higher in the masonry specimens strengthened with the manufactured meshes (with BCRs) compared with the masonry specimens with the equivalent commercial meshes. When the carbon fibre meshes are used, the resistance is about 5 times higher than the strength obtained in the reference unreinforced masonry and 3 times higher than when the meshes of glass fibres are used.
5. The masonry specimens present a more ductile behaviour when they are strengthened with manufactured meshes than when the commercial meshes are used. It seems that in

the designed meshes: (1) the damage is more controlled because there is a better load redistribution; (2) the ultimate deformation is increased and is accompanied by a reasonable residual strength. Notice that the commercial meshes have a very brittle behaviour. The presence of the polyester rods ensures high levels of deformation with reasonable residual load levels (between 50 and 90% of maximum).

6. The ductility factor calculated with respect to the displacement at peak load is greater in the specimens strengthened with the manufactured meshes than in the specimens reinforced with the commercial meshes. On the other hand, the ductility factor involving the ultimate displacement can only be measured in the case of strengthening with the manufactured meshes and it is higher when glass fibres are used in the BCRs.

7. As regards the behaviour of the specimen loaded under cyclic bending, it could be observed that the stiffness of the masonry strengthened with meshes of glass fibres decreases (exponential trend) more rapidly than the stiffness of the specimens reinforced with carbon fibre meshes (linear trend). This is related also to the greater nonlinearity exhibited by the masonry strengthened with the meshes with glass fibres.

8. It should be mentioned that the manufactured meshes with braided composite rods with a core composed of reinforcing glass fibres present a remarkably better post-peak behaviour than the specimens reinforced with the commercial meshes of glass fibres. Therefore, the meshes produced with glass fibre are advantageous in terms of their mechanical behaviour and can be custom-designed.

References

1. Lourenço P, Vasconcelos G, Medeiros P and Gouveia J. Vertically perforated clay brick masonry for loadbearing and non-loadbearing masonry walls. Construction and Building Materials 2010; 24 (11): 2317-2330.
2. Al-Chaar G, Issa M, and Sweeney S. Behavior of masonry-infilled nonductile reinforced concrete frames. Journal of Structural Engineering 2002. 128 (8): p. 1055-1063.
3. Lourenço PB, Pereira MFP, Leite JC and Costa, AC. Comportamento das paredes não estruturais a açoes sísmicas. Seminário sobre Paredes Divisórias: Passado, presente e futuro, P. B. Lourenço et. al (eds). Junho 2011.
4. Shing PB and Mehrabi AB. Behaviour and analysis of masonr y-infilled frames. Prog. Struct. Engng Mater 2002; 4 (3): 320-331.
5. EN-1998-1. Design of structures for earthquake resistance - Part 1: General rules, seismic actions and rules for buildings, Brussels: CNE. 1998.
6. Vintzileou E and Tassios TP. Seismic behaviour and design of infilled R.C. frames. European Earthquake Engineering 1989; 3(2): p. 22-28.
7. Soo-Yeon S, Feo L, Hui D. Bond strength of a near surface-mounted FRP plate for retrofit of concrete structures, Composite Structures, 95, 719-727, 2013.
8. Gómez JM. Innovative retrotting materials for brick masonry infill walls. Master's Thesis. University of Minho, Portugal; 2012.
9. Martins A. Soluções de reforço sísmico de paredes de alvenaria de enchimento. Master's thesis. Universidade do Minho, Portugal; 2013.
10. M Harajli, HE and San-Jose, JT. Static and Cyclic Out-of-Plane Response of Masonry Walls Strengthened Using Textile-Mortar System. Journal of materials in civil engineering 2010; 22 (11): p. 1171-1180.
11. Papanicolaou C, Triantafillou T and Lekka M. Externally bonded grids as strengthening and seismic retrofitting materials of masonry panels. Construction and Building Materials 2011; 25: p. 504–514.
12. Triantafillou TC and Papanicolaou CG. Textile Reinforced Mortars (TRM) versus Fiber Reinforced Polymers (FRP) as Strengthening Materials of Concrete Structures. FRPRCS; 2007; p. 99-118.
13. Papanicolaou CG, Triantafillou TC, Karlos K and Papathanasiou M. Textile-reinforced mortar (TRM) versus FRP as strengthening material of URM walls: in-plane cyclic loading. Materials and Structures 2007; 40: p. 1081–1097.
14. Papanicolaou CG, Triantafillou TC, Papathanasiou M. and Karlos K. Textile reinforced mortar (TRM) versus FRP as strengthening material of URM walls: out-of-plane cyclic loading. Materials and Structures 2008; 41: p. 143–157.
15. Koutas L, Bousias SN, and Triantafillou TC. Seismic strengthening of masonry infilled RC frames with TRM: Experimental study. ASCE Journal of Composites for Construction, DOI 10.1061/(ASCE)CC.1943-5614.0000507., 2014.

16. Koutas L., Triantafillou TC, and Bousias SN. Analytical modeling of masonry-infilled RC frames retrofitted with Textile Reinforced Mortar. ASCE Journal of Composites for Construction, DOI 10.1061/(ASCE)CC.1943-5614.0000553., 2014.
17. D´Ambrisi A, Mezzi M, Feo L, Berardi VP. Analysis of masonry structures stregthened with polymeric net reinforced cementitious matix materials, Composite Structures, 264-271, 2014.
18. Rupika, WK. Out of plane strengthening of unreinforced mansory walls using textile reinforced mortar systems. Master's thesis. University of National U of Singapore; 2010.
19. Bernat E., Gil L., Roca P. and Escrig C. Experimental and analytical study of TRM strengthened brickwork walls under eccentric compressive loading. Construction and Building Materials 2013; 44: p. 35-47.
20. Bernat E., Gil L, Roca P. and Escrig C. Experimental assessment of Textile Reinforced Sprayed Mortar strengthening system for brickwork wallettes. Construction and Building Materials 2014; 50: p. 226-236.
21. Greco F, Luciano R. A theoretical and numerical stability analysis for composite microstructures by using homogenization theory. Composites: Part B 42(3), 382-401 (2011).
22. Bruno D, Greco F, Luciano R, Nevone Blasi P. Nonlinear homogenized properties of defected composite materials. Computer and Structures 134, 102-111 (2014).
23. **Barretta R, Luciano R. Exact solutions of isotropic viscoelastic functionally graded Kirchhoff plates. Composite Structures 118, 448-454 (2014).**
24. **2. Apuzzo A, Barretta R, Luciano R. Some analytical solutions of functionally graded Kirchhoff plates. Composites: Part B 68, 266-269 (2015).**
25. **Barretta R, Luciano R. Analogies between Kirchhoff plates and functionally graded Saint-Venant beams under torsion. Continuum Mechanics and Thermodynamics 27(3), 499-505 (2015).**
26. **Barretta R, Feo L, Luciano R. Some closed-form solutions of functionally graded beams undergoing nonuniform torsion. Composite Structures 123, 132-136 (2015).**
27. **Barretta R, Feo L, Luciano R. Torsion of functionally graded nonlocal viscoelastic circular nanobeams. Composites: Part B 72, 217-222 (2015).**
28. **Barretta R, Feo L, Luciano R. Marotti de Sciarra F., Variational formulations for functionally graded nonlocal Bernoulli-Euler nanobeams. Composite Structures 129, 80-89 (2015).**
29. Cunha F. Desenvolvimento de uma estrutura com materiais fibrosos para ser utilizada como reforço de paredes de alvenaria. Master's Thesis. Universidade do Minho, Portugal; 2012.
30. Fangueiro R. Fibrous and composite materials for civil engineering applications. University of Minho, Portugal; 2011.
31. NP EN ISO 2062. Têxteis - Fios sob a forma de enrolamento. Determinação da força de rotura e alongamento de rotura. IPQ; 1997.

32. ASTM D5034-95. Standard Test Method for Breaking Strength and Elongation of Textile Fabrics (Grab Test). ASTM International, West Conshohocken, PA, 1995.
33. Martinelli E, Czaderski C. and Motavalli M. Modeling in-plane and out-of-plane displacement fields in pull-off tests on FRP strips. Engineering Structures 2011; 33 (12): p. 3715-3725.
34. Baena M, Torres L, Turon A and Barris C. Experimental study of bond behaviour between concrete and FRP bars using a pull-out test. Composites Part B: Engineering 2009; 40: p. 784-797.
35. Kashyapa J, Willisa CR, Griffitha MC, Inghamb JM, Masiac MJ. Debonding resistance of FRP-to-clay brick masonry joints. Engineering Structures 2012; 41: p. 186-198.
36. NP EN 772-1. Métodos de ensaios de blocos para alvenaria. Parte 1 - Determinação da resistência à compressão, Brussels: CNE; 2002.
37. EN 1015-11. Methods of test for mortar for masonry – Part 11: Determination of flexural and compressive strength of hardened mortar, Brussels: CNE; 1993
38. Abreu S. Metodologia de reforço de paredes de alvenaria de enchimento. Master's thesis. Universidade do Minho, Portugal; 2011.
39. BS EN 1052-2. Methods of test of masonry - Part 2: Determination of flexural strength, Brussels: CNE; 1999.